water

MDPI

Article

Explainable Artificial Intelligence Analysis of Simultaneous Anaerobic Nitrogen and Sulfur Removal in Anaerobic Sulfide Oxidation Bioreactor

Qaisar Mahmood [1,2,*], Uneb Gazder [3,*], Jing Cai [4], Imtiaz Ali Khan [5] and Yung-Tse Hung [6]

[1] Department of Environmental Sciences, COMSATS University, Abbottabad Campus, Abbottabad 22060, Pakistan
[2] Department of Biology, College of Science, University of Bahrain, Sakhir Campus, Zallaq 32038, Bahrain
[3] Department of Civil Engineering, University of Bahrain, Zallaq 32038, Bahrain
[4] College of Environmental Science and Engineering, Zhejiang Gongshang University, Hangzhou 314423, China; caijing@zjgsu.edu.cn
[5] Department of Entomology, KPK University of Agriculture, Peshawar 25000, Pakistan; imtiazkhanswb@gmail.com
[6] Department of Environmental Engineering, Cleveland State University, Cleveland, OH 44115, USA; y.hung@csuohio.edu
* Correspondence: drqaisar@cuiatd.edu.pk (Q.M.); ugazder@uob.edu.bh (U.G.)

Abstract

Biological wastewater treatment systems exhibit a wide range of operating conditions and influent substrate types. Artificial intelligence methods, particularly artificial neural networks (ANNs), are increasingly being employed to manage this complexity. This study uses ANN modeling to identify the key operational parameters that influence the efficacy of anaerobic sulfide oxidation (ASO) biotechnology, which simultaneously treats nitrite and sulfide. The ANN model was further analyzed through SHAP analysis to determine the key operational parameters. The dataset used in this study was derived from previously published operational data of ASO reactors. The results revealed that the sulfide-to-nitrite (S:N) ratio and hydraulic retention time (HRT) had the greatest impact on sulfide removal. In contrast, influent sulfide and nitrite concentrations had no effect on the prediction of effluent pH. While other parameters had a positive effect, HRT had a slight negative impact on effluent pH, with the S:N ratio having the most effect. Furthermore, while other factors contributed to sulfate generation, sulfide influent and HRT had a significant impact. Predicting nitrite-nitrogen (NO_2^--N) removal is mostly dependent on the S:N ratio and influent pH. To enhance ASO reactor performance for sulfide and nitrite removal, it is recommended to prioritize the optimization of the S:N ratio and HRT, as these parameters have the greatest impact on key treatment outcomes, including sulfide and NO_2^--N removal and sulfate formation.

Keywords: Anaerobic Sulfide Oxidation (ASO); Artificial Neural Networks (ANN); S:N Ratio; Hydraulic Retention Time (HRT); Nitrite-Nitrogen (NO_2^--N) Removal; wastewater treatment modeling

check for updates

Academic Editors: Gongduan Fan and Christos S. Akratos

Received: 27 April 2025
Revised: 10 June 2025
Accepted: 23 June 2025
Published: 24 June 2025

Citation: Mahmood, Q.; Gazder, U.; Cai, J.; Khan, I.A.; Hung, Y.-T. Explainable Artificial Intelligence Analysis of Simultaneous Anaerobic Nitrogen and Sulfur Removal in Anaerobic Sulfide Oxidation Bioreactor. *Water* **2025**, *17*, 1880. https://doi.org/10.3390/w17131880

Copyright: © 2025 by the authors. Licensee MDPI, Basel, Switzerland. This article is an open access article distributed under the terms and conditions of the Creative Commons Attribution (CC BY) license (https://creativecommons.org/licenses/by/4.0/).

1. Introduction

Industrial developments and urban settlements are unavoidable in modern times. However, such unchecked developments have threatened the future of humans, as evidenced by serious environmental consequences including global climate changes, soil

contamination, and most importantly the contamination of water resources. Among these undesirable consequences of non-sustainable development is water pollution. Water pollution caused by toxic pollutants is a global issue that affects the population in numerous ways, including its impact on direct consumption, agriculture, and recreational activities [1]. Various methods for the removal of pollutants from wastewater include chemical, photovoltaic, aerobic, and anaerobic pathways. Anaerobic methods utilize microorganisms to transform organic matter without the presence of oxygen, making them effective for treating high-strength wastewater.

Recent investigations have extensively focused on biotechnology for the concurrent removal of nitrogen and sulfur [2–6]. The use of biotechnology is essential for the well-being of ecosystems. This is because it transforms pollutants into benign substances, generates biodegradable materials from renewable sources, and develops environmentally safe manufacturing and disposal processes [2]. Some of these processes are conducted in the absence of oxygen, referred to as anoxic, such as denitrification for the removal of nitrate [7]. Another one of those technologies is anaerobic sulfide oxidation (ASO). The anoxic sulfide-oxidizing reactor is an up-flow reactor with biomass retention. The reactor is made of Perspex with a working volume of 1.3 L. The synthetic influent is pumped through a peristaltic pump from the 5 L influent vessel to the reactor. The flow rate can vary between 0.6 and 12.5 L per day, which provides the possibility of operating at HRTs between 2.0 and 0.1 days. A recycling pump is used in order to mix the influent (substrate) and sludge (biocatalyst) well and hence to decrease possible substrate inhibition. The process can be controlled by changing the ratio of recycling flow to the influent flow and the temperature of the reactor between [2]. One of the challenges with the employment of ASO technology is the variation in reactor performance due to the intensity of shock loads. The effect of shock loading is directly proportional to the intensity of the shock loads. The reactor performance is observed to be stable at a relatively lower intensity (1.5 times shock load), while it shows considerable disturbance at a higher intensity (higher than 2.0 times shock load). The effluent sulfide-sulfur concentration was also found to be another sensitive parameter affecting the steady state of the reactor [4].

The ASO reactor efficiently managed elevated influent quantities of sulfide (1920 mg/L) and nitrite (2265.25 mg/L). A 0.10-day hydraulic retention time (HRT) yielded peak loading rates of 13.84 kgS/(m^3·d) and 16.311 kgN/(m^3·d). A stoichiometric analysis indicated incomplete oxidation of sulfide, leading to the formation of elemental sulfur, attributed to a low sulfide-to-nitrite ratio of 0.93 [2]. HRT did not influence sulfide removal but significantly affected nitrite removal. The reactor withstood a 0.10-day hydraulic retention time, but performance declined when it dropped to 0.08 days [2,3].

Mahmood et al. [3] reported that sulfide removal efficiency in ASO was not significantly affected when HRT was lowered from 1.0 to 0.10 days. However, reducing HRT to 0.08 days negatively impacted reactor performance. Nitrite removal was significantly influenced by changes in HRT, indicating the reactor's adaptability to operational adjustments [4]. The importance of aerobic polishing following the ASO reactor for achieving effluent standards was emphasized, with results showing successful compliance after 12 h of aeration at dissolved oxygen (DO) levels below 1.0 mg/L [4].

Artificial neural network (ANN) modeling proved effective for the performance prediction of the ASO reactor, achieving good agreement between predicted and observed values with correlation coefficients of 0.96 for nitrite and 0.98 for sulfide [5]. Further optimization of the ASO reactor via ANN and Genetic Algorithm (GA) models enhanced performance under varying influent concentrations and operational conditions [5]. Similarly, simultaneous removal of nitrogen and sulfur has been investigated in mixed culture bioreactors, demonstrating efficient performance under controlled conditions [6]. Researchers have also

applied constructed wetlands (CWs) to treat wastewater containing sulfide and nitrogen compounds. CWs offer low-cost and sustainable treatment solutions by leveraging natural processes such as microbial activity, plant uptake, and sedimentation [8–11].

In recent years, machine learning (ML) techniques have shown great potential in optimizing wastewater treatment processes, including sulfide and nitrogen removal [12]. Among these, artificial neural networks (ANNs) have proven to be a powerful tool for modeling complex, non-linear relationships inherent in biological treatment systems [13,14].

ANN models mimic the functioning of biological neural systems to learn patterns in data, enabling them to predict system behavior under different operational conditions [13,15]. They have been applied successfully in various domains, including speech recognition [16,17], natural language processing [18–20], autonomous driving [21], medical diagnosis [22], and financial prediction [23].

Recently, researchers have increasingly applied ANNs to environmental engineering problems, particularly in water and wastewater treatment [24,25]. In this study, we utilized ANN modeling to predict the performance of an ASO reactor for the simultaneous removal of sulfide and nitrite under various operational conditions. Additionally, we employed SHapley Additive exPlanations (SHAP) analysis to interpret the contribution of different input variables to the reactor performance prediction. The use of SHAP analysis with ANNs is referred to as Explainable AI or XAI. Its application in the environmental field, despite its popularity in other fields, is rather limited. The limited literature found thus far shows that this approach increases the robustness of the models, as well as their generalizability. Moreover, it improves the interpretability of the results. Consequently, higher accuracy and interpretability aid decision-making ability, which could be vital for wastewater treatment systems [26,27].

The applications of XAI found thus far in the field of water treatment are all recent, which shows the popularity of this approach among modern researchers. More prominently, they deal with the prediction of water quality; such examples include [28–30]. Another field of application is water demand management and prediction [31]. With regard to the use in wastewater treatment, Nasir and Li [32] have used this approach successfully for sludge prediction through employment of various tree-based models. Sludge monitoring was also conducted through image detection by applying deep learning [33]. With regard to the tree models, they were also used in other studies for optimizing the parameters of wastewater treatment plants for cost minimization [34]. One of the very few studies found to focus on the chemical parameters of treated wastewater is by [35].

It is evident from the above that previous research on the use of ANNs and XAI in microbially controlled biotechnologies is scarce. Artificial intelligence techniques are now widely used to reap the benefits of modern technological progress. The artificial neural network model is expected to aid in identifying the important elements influencing the ASO biotechnology that treats nitrite and sulfide at the same time. Based on these findings, this study employs ANN models to predict the removal of pollutants from wastewater subjected to ASO treatment technology. The data for this study was taken from previously published works of [2–6], and the focus of the study was kept on the modeling aspect. The models were subjected to SHAP analysis for determining the key parameters and their impact on pollutant removal. XAI lends itself as an effective and efficient method for obtaining accurate predictions of results as well as for determining the impacts of variables despite limitations of data and prior information about them.

The comparative analysis provided by the SHAP analysis, between different parameters, cannot be achieved through other traditional methods with the above-mentioned limitations. This type of research is non-existent in the field of ASO reactor performance prediction. The prediction model and its findings provide a solid basis for the application

and improvement of the ASO method by exploring the values of operational factors beyond their known ranges.

2. Methods of Analysis

2.1. Data Collection

The ASO reactor is an up-flow mode that retains biomass. The reactor is composed of Perspex with a working volume of 1.3 L. The synthetic influent is pumped from the 5 L influent vessel to the reactor via a peristaltic pump (Longer Pump YZ1515X, Hebei, China). The hydraulic retention time (HRT) of this influent pump is determined by the pump flow rate, as the residence time is defined as the volume–flow rate ratio. The flow rate can vary between 0.6 and 12.5 L per day, allowing for HRTs of 2 to 0.1 days. A recycling pump is employed to ensure proper mixing of the influent (substrate) and sludge (biocatalyst), hence reducing the possibility of substrate inhibition. The recycling flow-to-influent flow ratio is fixed at around 2.5–3. The influent flow rate is, however, identical to the actual effluent flow rate because the withdrawal threshold is 1.3 L. The temperature of the reactor can be regulated using a thermostat between 20 °C and 70 °C, though the normal operational temperature is 35 °C, as is typical of the ASO process. The data obtained from the operation of various aspects of ASO reactors have been published previously [2–6] and were employed for artificial neural network studies.

2.2. Artificial Neural Network

ANN models work with the combination of three types of layers, which are shown in Figure 1 and described as follows:

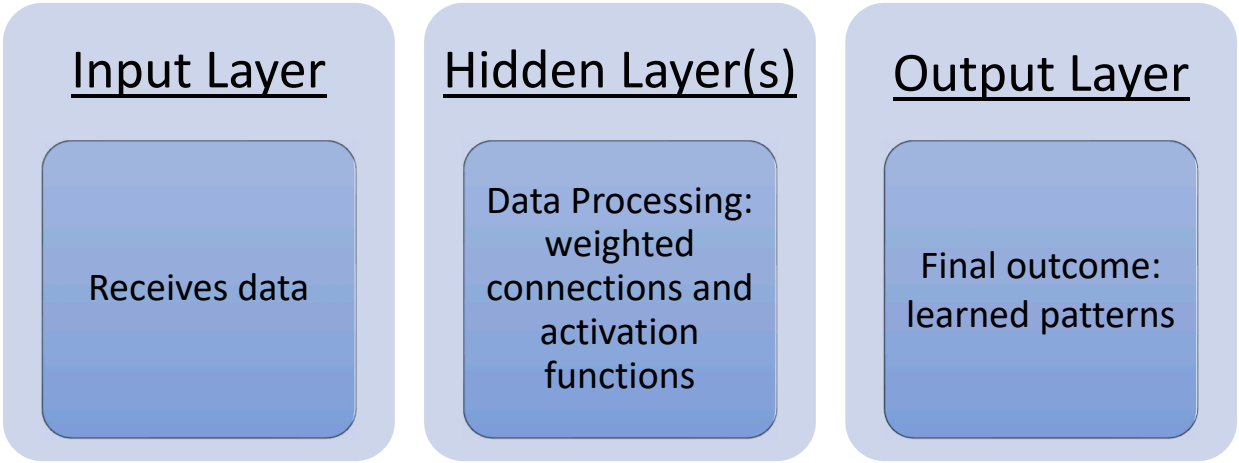


Figure 1. Working flow of artificial neural network models.

1. Input Layer: Receives input data, which is typically normalized or standardized.
2. Hidden Layers: Process the input data through a series of weighted connections and activation functions, capturing complex patterns.
3. Output Layer: Produces the final output based on the learned patterns. The number of nodes in this layer depends on the type of task (e.g., classification, regression) [24].

During training, the network adjusts the weights of connections to minimize the difference between predicted and actual outputs (the loss function). This process, known as backpropagation, involves iteratively updating weights using optimization algorithms like gradient descent. Once trained, the neural network can make predictions on new, unseen data [25].

In conclusion, neural network models are a powerful tool in the field of artificial intelligence, with a wide range of applications and the ability to learn complex patterns

from data. There have been previous studies in which ANN models have been used for the prediction of chemical processes in water treatment, and they have proven to perform better than statistical techniques such as linear regression [26]. Having said that, their application in the field of chemical engineering biology is rather limited. Hence, this study is an attempt to capitalize on the positive aspects of ANN models to improve the prediction ability and understanding of chemical processes associated with water treatment.

2.3. SHAP Analysis

SHAP (SHapley Additive exPlanations) analysis is a powerful method used to explain the output of machine learning models by attributing the prediction to its individual features. It is based on the concept of Shapley values from cooperative game theory, which assigns a value to each feature representing its contribution to the prediction [27].

SHAP begins by calculating Shapley values, which quantify the impact of each feature on the model's prediction. It considers all possible feature combinations and how each feature contributes to the prediction when added to a subset of features. The calculation of SHAP values can be performed using Equation (1):

$$SHAP(v) = \frac{1}{p}\sum_{s} \frac{[v(s \cup \{m\}) - v(s)]}{\binom{p-1}{k(s)}},\ m = 1, 2, 3, \ldots\ldots p \quad (1)$$

where v is the function or model for which *SHAP* values are calculated, m is the member for which the current *SHAP* value is calculated, s denotes the possible subset of the variables and $s \cup \{m\}$ shows the value of the model with the addition of member m. The Shapley values are then used to rank the features based on their importance. Features with higher Shapley values are considered more important as they have a greater impact on the model's output [36].

SHAP provides a clear and interpretable explanation of the model's predictions, making it easier to understand the model's behavior. It allows for both global and local interpretation, providing insights into how each feature affects individual predictions as well as the overall model behavior. It can also be used to compare the importance of features across different models, helping in model selection and feature engineering. SHAP is robust to correlated features and provides reliable explanations even in complex models like ensemble methods and neural networks [37]. Due to the above advantages, SHAP has been used in a variety of fields such as prediction of skin cancer, identification of manipulations in an image, evaluation of industrial internal security, and many others [38].

The above discussion clearly shows that SHAP analysis is a valuable tool for understanding and interpreting machine learning models, providing insights into feature importance and model behavior, and finding applications across various industries. This is the reason for employing it in the current study.

3. Results

3.1. ANN Models

There is a wide variety of ANN techniques and approaches which have been adopted by researchers. This study limits itself to the use of a multilayer perceptron (MLP), which is a popular type of ANN model. The network weights were optimized using a two-step procedure including backpropagation and conjugate gradient methods applied in a series with the same order. The input and output variables for each model developed in this study are shown in Figures 2–6. They were normalized using Equation (2) [39].

$$X_N = \frac{(X - X_{min})}{(X_{max} - X_{min})} \quad (2)$$

The sum of squared errors was minimized to find the appropriate weights and select the best network architecture. The former included optimizing the number of hidden layers and the number of neurons in each of those layers. The hidden-layer neurons had a hyperbolic activation function, while for the output layer, it was logistic. STATISTICA version 14.1.0 (by STATSOFT Inc., Hamburg, Germany) was used for this analysis. The accuracy of the models was tested using three different parameters, namely, correlation coefficient (CC), root mean square error (RMSE) and mean absolute percentage error (MAPE). The available dataset was divided into three parts; 50% was randomly selected for training the model and 25% was randomly selected for selecting the best model parameters, while the remaining was used for testing the model. The approach is similar to that found in recent research in similar areas [27]. The weights for each ANN model are included in the Appendix A for readers interested in replicating the results. The above methodology of testing the model on an independently selected test dataset, along with the application of various accuracy parameters to all datasets, gives fair evidence about the reliability of the models (see Tables 1–5).

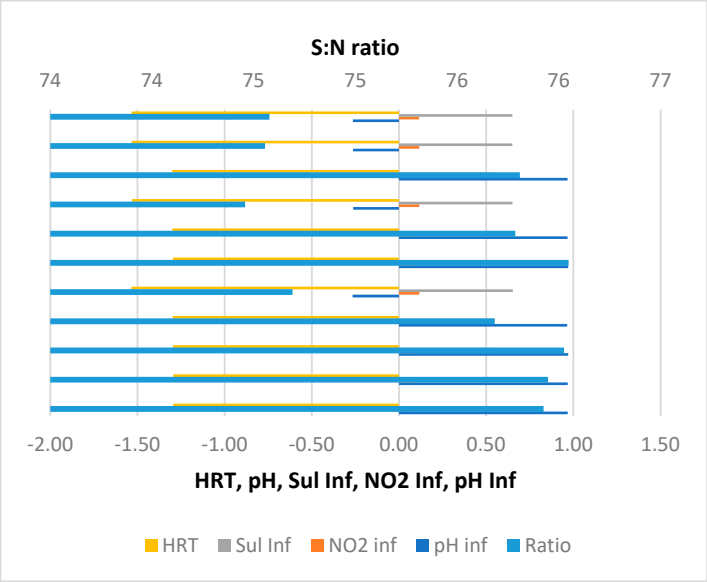


Figure 2. Feature importance for sulfide removal prediction model.

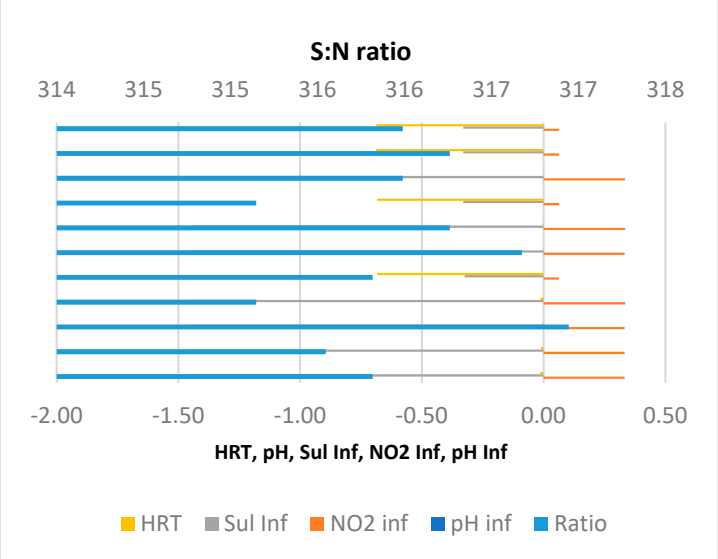


Figure 3. Feature importance for sulfate formation prediction model.

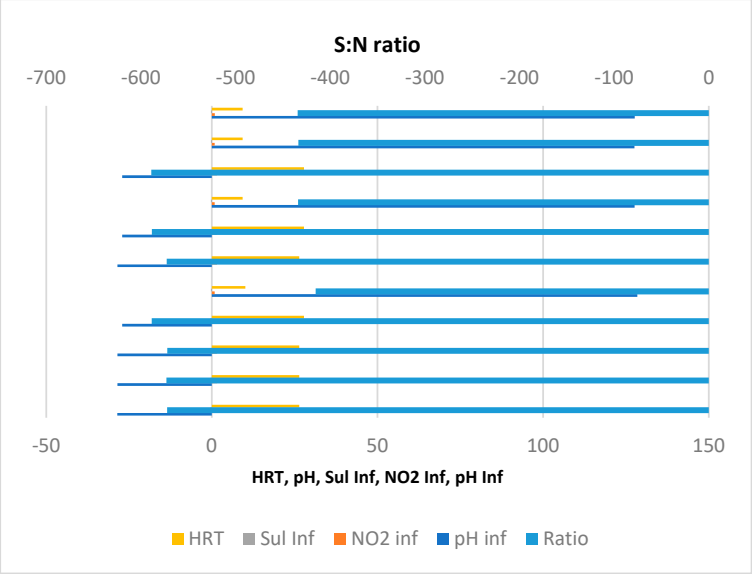


Figure 4. Feature importance for NO_2-N removal prediction model.

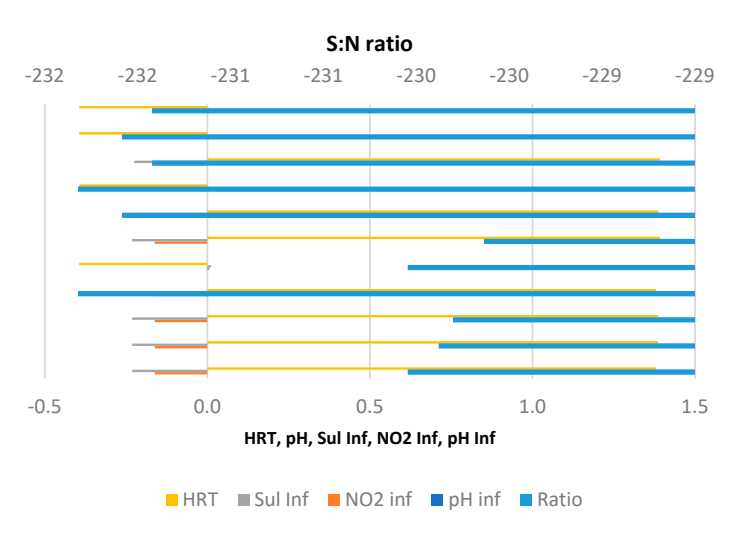


Figure 5. Feature importance for NH_4-N formation prediction model.

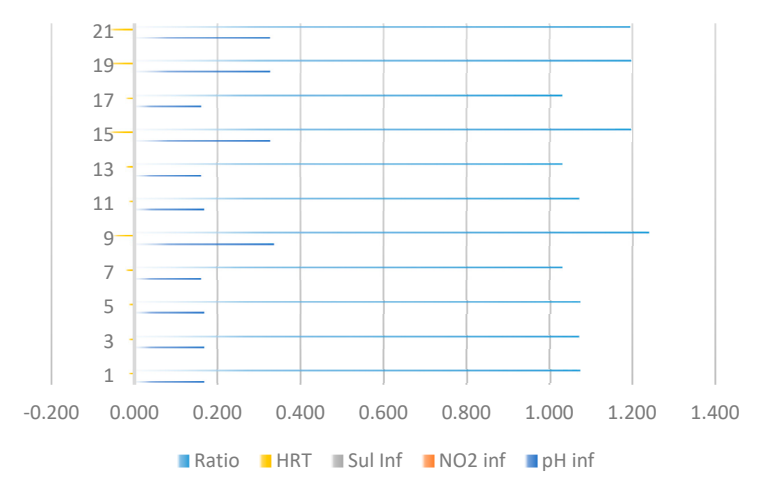


Figure 6. Feature importance for pH effluent prediction model.

Table 1. Accuracy of sulfide removal prediction model.

Dataset	RMSE	MAPE	CC
Training	11.48	2.26	0.99
Selection	20.71	2.79	0.99
Test	14.29	1.36	0.99

Table 2. Accuracy of sulfate formation prediction model.

Dataset	RMSE	MAPE	CC
Training	83.47	106.04	0.80
Selection	95.88	57.26	0.68
Test	111.23	43.46	0.56

Notes: Not good results. Recommended to be modeled using other techniques such as deep learning.

Table 3. Accuracy of NO_2-N removal prediction model.

Dataset	RMSE	MAPE	CC
Training	43.53	4.28	0.99
Selection	63.92	4.10	0.99
Test	53.77	5.01	0.99

Table 4. Accuracy of NH_4 formation prediction model.

Dataset	RMSE	MAPE	CC
Training	20.55	N/A	0.95
Selection	15.52	N/A	0.89
Test	47.70	N/A	0.64

Table 5. Accuracy of effluent pH prediction model.

Dataset	RMSE	MAPE	CC
Training	0.22	1.97	0.93
Selection	0.28	2.50	0.90
Test	0.24	2.14	0.92

Most of the models showed acceptable RMSE and CC values for all dataset types (training, selection and test). More importantly, the models for sulfide and NO_2-N removal provided a high CC across all datasets, which is the most important result of the ASO process. RMSE and CC are more stable parameters as compared to MAPE. It is possible to calculate them for any dataset, even with large ranges or values of 0 magnitude. The sulfide removal prediction model was the best in terms of both the CC between predictions and actual values and MAPE. The models for predicting the formation of sulfate and NH_4 showed a large variation in accuracies between different datasets, which raises a question about their robustness. The accuracies of the present models are generally better than those obtained by Mahmood et al. [2,3], including those models which are mentioned above. The possible reasons could be the implementation of a two-stage learning process and the use of two hidden layers, wherever appropriate. Moreover, the present study evaluates the models in a better way by using it on test datasets and including multiple parameters. In conclusion, it can be said that the models developed in this study are more accurate and

the results are more reliable than previous relevant studies due to testing on independent datasets and employing various accuracy parameters.

3.2. SHAP Analysis Outcome

It was discovered that the S:N ratio and HRT had the greatest influence on predicting sulfide removal (Figure 2 and Table S1). The average SHAP value for the S:N ratio was 75 (Table S1), as depicted in the secondary *x*-axis of Figure 2. This implies that all variables except HRT could boost sulfide removal, which makes sense because a lower HRT means less time available for the sulfide removal process.

According to Figure 3, the S:N ratio and sulfide influent had the greatest influence on the prediction of sulfide removal. Sulfide influent and HRT both had a detrimental impact on sulfate formation, whilst other variables had a beneficial impact.

As evident in Figure 4, the S:N ratio and influent pH had the highest impact on the prediction of NO_2-N removal. The S:N ratio and sulfide influent had negative impacts on the removal of NO_2-N, while other variables had a positive impact on it.

As shown in Figure 5, the S:N ratio and HRT had the highest impact on the prediction of NH_4^+ formation. The impact of influent pH was almost zero in this case (Table S4). From the other remaining variables, only HRT had a positive impact, which could be linked to the time of the chemical process.

Figure 6 illustrates that sulfide and NO_2^- for the influent had almost no impact on the prediction of effluent pH. HRT had a small negative impact on the predictions, while the remaining variables had a positive impact on it, with the impact of the S:N ratio being the highest. Similar findings have been found for pH levels for gas treatment processes with an impact of the ratio [40].

Table 6 illustrates that the influent substrate ratio significantly affected all forecast types. HRT exerted a more significant impact on most models. Conversely, influent factors like pH and NO_2- significantly affected the predictions of NO_2-N removal.

Table 6. Comparison of SHAP values for all models.

Predictions	pH Influent	NO_2 Influent	Sulfide Influent	HRT	Ratio
Sulfide Removed	0.52	0.10	0.59	−1.38	75.41
Sulfate Formed	0.00	0.24	−1.04	−0.25	315.96
NO_2-N Removed	28.73	1.28	−0.40	20.63	−524.81
NH_4-N Formed	0.00	−0.10	−0.14	0.74	−230.82
pH Effluent	0.23	0.00	0.00	−0.03	1.11

3.3. Critical Parameters Affecting N and S Removal

Researchers discovered that artificial neural networks can accurately estimate effluents from anoxic sulfide oxidation processes based on influent data. XAI provides accurate predictions coupled with greater interpretability of the model results. Hence, the parameters affecting the performance of the process are known and their impacts are determined. Consequently, it can be used for better decision making. The current technique accurately predicts effluent pH, nitrite, and nitrogen contents in ASO reactors. Nonetheless, the model cannot predict the formation of sulfide and sulfate throughout the ASO process. The observed oscillations during the experiment make the ANN model's erratic behavior regarding sulfate formation understandable.

In our real trial [2,3], HRT had little effect on the percentage of sulfide elimination. When the hydraulic retention duration was reduced from 1.5 to 0.10 days, the effluent sulfide concentration remained continuously below 2 mg/L, with a clearance rate of more

than 99.16%. The process abruptly ended when the hydraulic retention period was reduced to 0.08 days, resulting in a 96.66% fall in sulfide removal efficiency [2]. When reduced, sulfide can be oxidized to sulfate or elemental sulfur in the presence of an electron acceptor. McNeice [41] observed that lower sulfide-to-oxygen ratios resulted in the formation of both sulfur and sulfate; however, in oxygen-limited conditions, thiosulfate emerged as the predominant product. Sun et al. [42] found that sulfide concentration and input sulfide–nitrate ratios were important determinants in sulfide oxidation. The optimal conditions for manufacturing sulfur as the principal product were proposed to be sulfide concentrations below 9 mmol/L and sulfide-to-nitrate ratios of 1.6 and 2.5. Mahmood et al. [2] discovered that higher influent sulfide-sulfur loading resulted in elemental sulfur being the predominant product of sulfide biooxidation when nitrite was used as the electron acceptor. The inhibitory sulfide levels could prompt the growth of sulfur-, iron-, nitrate- and nitrite-metabolizing microorganisms [43]. The experiment, which used an ASO reactor with different hydraulic retention times (HRTs), found that nitrite removal was responsive to changes in HRT. The ANN model properly predicted nitrite removal. The model may be validated using estimates for nitrite elimination. The speeds of biological processes follow laws like those governing pure substances. The reaction rates for biochemical processes vary depending on plant conditions and environmental variables such as temperature and pH.

Dependence is sometimes non-monotonic, with certain processes emerging exclusively at specific dosage levels. Diverse inputs to the ASO reactor, including sulfide and nitrite, can result in sulfate or sulfur (not measured), dinitrogen gas, and trace amounts of ammonium. In ANN analysis, hydraulic retention time (HRT) and pH are considered essential input parameters for predicting reactor output. As a result, four input variables—sulfide, nitrite, pH, and hydraulic retention time (HRT)—can influence the generation of four outputs: sulfate, sulfur, nitrogen, and ammonium. Yuan et al. [43] found no significant difference in nitrate-nitrogen (NO_3^--N) levels between pH levels 6 and 7.5 and hydraulic retention times (HRTs) of 7.41 to 6.83 h. Nonetheless, lowering the HRT caused an increase in elemental sulfur accumulation. A lower pH, especially near 7, encouraged the buildup of elemental sulfur. A second pH drop resulted in a modest rise [44].

In the current study, HRT had a minor negative effect on outcome prediction, whereas the other variables had a favorable influence, with the impact ratio being the most pronounced. The efficacy of NO_2^--N removal was significantly affected by the influent's pH and nitrite contents.

The ANN prediction shows that the influent S:N ratio and HRT have the greatest influence on NH_4 production prediction. The technical impediment to the commercially practical adoption of this method for sour waste treatment may be related to substrate and product inhibition, which explains the partial oxidation of sulfide [45]. Sulfide is harmful to *Thiobacillus denitrificans* because it acts as an inhibitory substrate. The practical effect is that reactor systems designed to handle sulfide-laden waste must be sulfide-limited, which ensures that the steady-state concentration of sulfide in the bulk liquid remains below inhibitory limits. Furthermore, reactor systems must be adequately mixed to avoid significant sulfide concentration gradients, which might lead to isolated zones with inhibitory sulfide levels [45]. In the current study, it was discovered that sulfate concentrations more than 250 mg/L, together with a higher reactor pH, may have had inhibitory effects (product inhibition) on the complete oxidation of sulfide to sulfate. This was the case observed in the present study, which shows that the reactor was in the transient state. The higher removal rates observed in this investigation at various nitrite-to-sulfide influent molar ratios suggest that sulfide oxidation is incomplete, resulting in the generation of elemental sulfur. It was found in previous studies that sulfate oxidation

is primarily affected by the liquid-to-solid ratio, followed by the inlet SO_2 concentration, with temperature having the lowest impact among them [46]. In this regard, a wide variety of techniques have been applied to enhance the oxidation process for the removal of unwanted substances. Among them, photo-assisted techniques and electrochemistry have been found to be very effective [47]. However, their integration with the ASO process is still to be explored.

T. denitrificans produces sulfate through the aerobic or anoxic oxidation of sulfides (with nitrate). Sulfate concentrations of more than 250 mg inhibit *T. denitrificans* [48]. This is most likely due to increased ionic strength rather than the inherent inhibition of sulfate. Product inhibition limits the operation of both batch and continuous reactors. Sulfate accumulation in batch systems can have an impact on the batch cycle duration. In a continuous system, the dilution rate determines the sulfate concentration at a steady state; hence, for any given sulfide input rate, the reactor volume or hydraulic throughput is determined by the sulfate concentration needed in the culture [48,49]. Our previous research into concurrent sulfide and nitrite elimination at an influent molar ratio of 1.17 revealed that sulfide oxidation was not fully achieved, with approximately 10–11% of sulfide removal attributed to autooxidation caused by trace amounts of dissolved oxygen in the influent wastewater [3].

The simultaneous oxidation of sulfide and reduction of nitrite is a promising biological method for wastewater treatment, providing a sustainable and cost-effective way to eradicate both sulfur and nitrogen contaminants at once. This method uses microbes to turn sulfide into less harmful forms, like elemental sulfur or sulfate, while also turning nitrite into nitrogen gas. This solves the problem of both sulfurous and nitrogenous pollution in different types of industrial and agricultural wastewater. The sulfide-to-nitrite ratio (S:N ratio), pH, ammonium concentration, and influent sulfide concentration are just a few of the environmental and operational factors that have an impact on this process's efficiency and stability. These factors also have a significant impact on the microbial community structure and metabolic pathways. Understanding these features and their complex interrelationships is critical for improving the efficacy and dependability of sulfide oxidation and nitrite reduction systems in actual applications. Mahmood [2,3] discovered four input variables (sulfide, nitrite, pH, and HRT) that result in three outputs (sulfate, nitrogen, and ammonium).

4. Conclusions

The present investigation on the SHAP (SHapley Additive exPlanations) analysis of data obtained from an anaerobic ASO reactor treating sulfide and nitrite led to the following key findings.

The efficiency and stability of the ASO biotreatment process are influenced by a complex interaction of environmental and operational factors, including the sulfide-to-nitrite ratio (S:N ratio), pH, ammonium concentration, and influent sulfide concentration, all of which have a significant impact on the microbial community structure and metabolic pathways.

The S:N ratio and HRT were found to have the greatest influence on the prediction of sulfide removal efficiency. The positive impact of the S:N ratio on the removal rates suggests that sulfide oxidation is incomplete, resulting in the generation of elemental sulfur. Sulfide and nitrite concentrations in the influent had minimal effect on predicting the effluent pH, while the S:N ratio had the highest positive impact. The higher removal rates observed in this investigation at various nitrite-to-sulfide influent molar ratios suggest that sulfide oxidation is incomplete, resulting in the generation of elemental sulfur. Sulfide influent and HRT showed a detrimental effect on sulfate formation, whereas other variables contributed positively. The S:N ratio and influent pH were the most influential factors in predicting NO_2^--N removal.

To optimize reactor performance for sulfide and nitrite removal, it is recommended to prioritize fine-tuning the S:N ratio and HRT, as these parameters significantly influence key performance indicators like sulfide and NO_2^--N removal, as well as sulfate formation. The SHAP analysis showed that both these parameters have opposite effects on sulfide removal and nitrate formation. However, the impact on nitrate was higher than on sulfide removal. Hence, it could be said that a focus on nitrate removal would have a slightly negative impact on sulfide removal.

This study found that pH and HRT have significant impacts on wastewater treatment plants, but their accuracy varies due to high variation in the data. To improve the results, meta-heuristic or deep learning models may be employed. Future research should include real-world validation and explore microbial dynamics under varying environmental parameters. Advanced oxidation techniques could also be explored to reduce unnecessary substances in the system.

Supplementary Materials: The following supporting information can be downloaded at: https://www.mdpi.com/article/10.3390/w17131880/s1, Supplementary Table S1. Shapely Values for Sul Removed Prediction Model. Supplementary Table S2. Shapely Values for Sulfate Formed Prediction Supplementary Table S3. Shapely Values for NO_2-N Removal Prediction Model. Supplementary Table S4. Shapely Values for NH_4-N Formed Prediction Model. Supplementary Table S5. Shapely Values for pH Effluent Prediction Model.

Author Contributions: Methodology, Q.M. and J.C.; Software, U.G.; Formal analysis, Q.M., U.G. and Y.-T.H.; Investigation, Q.M. and J.C.; Resources, J.C. and Y.-T.H.; Data curation, I.A.K. and Y.-T.H.; Writing—review & editing, I.A.K. and Y.-T.H. All authors have read and agreed to the published version of the manuscript.

Funding: This research received no external funding.

Data Availability Statement: Data is contained within the article.

Conflicts of Interest: The authors have no conflict of interest.

Appendix A

Table A1. Neural Network Weights for Sul Removed.

Layer	Weight	Neuron 1	Neuron 2	Neuron 3	Neuron 4	Neuron 5
2	Threshold	0.734895	0.14332	0.609806	0.553195	0.734895
	W1	0.125874	−0.01108	−0.123308	−0.079186	0.125874
	W2	−0.184298	−0.42810	0.045927	0.033984	−0.184298
	W3	1.033897	−1.34412	0.546967	0.886106	1.033897
	W4	−0.000431	0.10962	0.073516	−0.002870	−0.000431
	W5	−0.138503	−0.06813	0.118240	0.065655	−0.138503
3	Threshold	0.441433	0.757272	−0.807444	0.331590	
	W1	−0.382654	1.009133	0.122110	−0.342085	
	W2	0.622816	−0.195391	−0.185834	1.268736	
	W3	−0.000892	0.578166	0.226279	0.142720	
	W4	−0.554850	0.874384	0.136965	−0.431479	
4	Threshold	0.24543				
	W1	−1.24951				
	W2	2.17651				
	W3	0.31365				
	W4	−1.24422				

Table A2. ANN Weights for Sul Formed.

Layer	Weight	Neuron 1	Neuron 2	Neuron 3	Neuron 4	Neuron 5	Neuron 6	Neuron 7
2	Threshold	−0.25402	−0.856211	−1.03164	1.283578	−2.47577	−0.252317	−0.177186
	W1	−0.74013	0.388996	0.41232	2.338687	−1.48365	−0.511173	−0.815234
	W2	−1.03677	1.290209	−0.00255	0.512451	0.09562	2.200229	3.938584
	W3	0.59293	−0.259599	0.24495	0.864413	−1.83519	0.006008	0.501213
	W4	0.60005	0.422904	−0.09469	−0.453886	0.74836	0.323768	−0.537115
	W5	−0.25402	−0.856211	−1.03164	1.283578	−2.47577	−0.252317	−0.177186
3	Threshold	−0.33212						
	W1	0.99034						
	W2	−0.46433						
	W3	0.62852						
	W4	2.45765						
	W5	2.68945						
	W6	−1.37689						
	W7	−2.75697						

Table A3. ANN Weights for NO2-N Removed.

Layer	Weight	Neuron 1	Neuron 2	Neuron 3	Neuron 4	Neuron 5	Neuron 6	Neuron 7	Neuron 8	Neuron 9	Neuron 10	Neuron 11	Neuron 12
2	Threshold	0.77412	0.456014	−0.031473	1.181602	0.485206	−0.612913	−0.179313	0.175743	−0.097188	−0.226884	−0.832653	0.315406
	W1	−0.56876	0.218188	−0.370007	0.076601	0.389217	−0.788336	−0.660659	−0.368171	−0.085167	0.579430	−0.104846	−0.306158
	W2	−1.05890	0.881294	−0.426706	0.422553	0.034106	−0.372050	0.987558	−0.399188	0.083581	0.567741	0.968475	0.514185
	W3	0.67022	−0.472024	0.008493	0.797143	−0.066656	0.577456	−0.153783	−0.835811	−0.054092	0.712828	−0.360356	0.792020
	W4	0.15358	0.420844	−0.852411	0.647223	0.388734	0.297250	−0.064015	1.029580	−0.037335	−0.435801	0.572786	−0.270927
	W5	0.72592	−0.688227	−0.644760	0.031604	0.843404	0.737271	0.381358	−0.907832	−0.003515	0.147512	0.164616	−0.826120
3	Threshold	0.070233	0.297925	0.205179	0.572240	0.867277	−0.294691						
	W1	0.515142	−0.922552	−0.958962	−0.618872	−0.064719	0.331149						
	W2	−0.231970	−0.207528	−0.229932	0.100993	−0.220813	0.676270						
	W3	0.706281	−0.999298	−0.016030	−0.575983	0.479162	0.755654						
	W4	1.051252	0.090775	0.161735	−0.345654	−0.324120	−0.585142						
	W5	0.217223	0.351567	0.371642	−0.201453	−0.120096	−0.026625						
	W6	−0.340079	0.637359	0.495911	−0.907844	0.258160	−0.279963						
	W7	−0.295758	−0.764562	0.539758	0.396139	−0.686912	1.006009						
	W8	−0.967223	0.141457	−0.226930	0.673835	−0.118477	0.127589						
	W9	−0.623107	0.569373	0.464128	−0.903109	−0.795511	−0.754020						
	W10	0.949142	0.143367	−0.428181	0.210982	0.444387	0.501235						
	W11	−0.011089	0.547601	−0.160073	0.244322	−0.208659	−0.129049						
	W12	0.595417	0.681863	0.241115	0.849668	0.018242	−0.819467						
4	Threshold	0.756666											
	W1	0.406573											
	W2	0.709643											
	W3	0.599181											
	W4	0.420095											
	W5	−0.735801											
	W6	0.640824											

Table A4. ANN Weights for NH4-N Formed.

Layer	Weight	Neuron 1	Neuron 2	Neuron 3	Neuron 4	Neuron 5	Neuron 6	Neuron 7	Neuron 8	Neuron 9	Neuron 10	Neuron 11
2	Threshold	7.58530	−0.59720	0.206648	−2.43860	0.540810	−1.39966	1.286364	−1.73442	0.925801	1.053922	0.96235
	W1	4.34586	−1.79148	−0.426081	0.03309	0.295972	−0.23042	−0.211485	0.82877	0.303824	−0.126191	0.97313
	W2	3.12185	−1.72340	0.059979	0.60584	0.176060	−0.17481	−0.116214	1.10853	0.539688	−0.032217	1.15592
	W3	−2.02107	2.56593	0.213490	0.18549	0.839211	0.09246	−0.324752	−0.22160	−0.054978	−0.174338	−0.53851
	W4	1.86011	3.79056	−0.164943	−0.09287	0.878869	0.69389	−0.378472	−0.47720	0.264341	−0.072815	−2.03750
	W5	7.58530	−0.59720	0.206648	−2.43860	0.540810	−1.39966	1.286364	−1.73442	0.925801	1.053922	0.96235
3	Threshold	−0.65140										
	W1	5.68331										
	W2	−2.16740										
	W3	0.31994										
	W4	−1.65635										
	W5	−0.57112										
	W6	1.30191										
	W7	−0.96438										
	W8	1.50757										
	W9	−0.60192										
	W10	−0.69405										
	W11	−2.87544										

Table A5. ANN Weights for pH Effluent.

Layer	Weight	Neuron 1	Neuron 2	Neuron 3	Neuron 4	Neuron 5	Neuron 6	Neuron 7	Neuron 8	Neuron 9	Neuron 10
2	Threshold	1.05823	0.133405	0.897519	−0.928437	0.13166	0.430889	0.496107	0.792288	−0.338700	−1.18038
	W1	−0.17187	−0.647502	−0.279515	−0.130696	−1.23356	−0.318732	1.171366	0.455697	−0.528742	−0.70187
	W2	−1.27256	−0.184953	1.480335	0.304847	−1.25112	2.287030	1.179459	−0.598229	0.184459	−1.15570
	W3	1.77981	0.047005	1.408471	0.736807	0.61838	0.275934	−0.098645	0.840573	−0.026089	−0.35959
	W4	−0.14882	−0.240262	−0.329721	0.468579	1.37652	1.029025	0.532582	0.264717	0.967747	−0.42022
	W5	1.44024	0.351557	−0.041667	0.495466	0.34486	0.170214	−0.535821	0.777898	−0.297486	1.00858
3	Threshold	1.72206									
	W1	−0.43139									
	W2	−1.29787									
	W3	0.55378									
	W4	−1.65740									
	W5	−1.48795									
	W6	1.56548									
	W7	0.91893									
	W8	−0.70073									
	W9	−1.42133									
	W10	1.72206									

References

1. Huang, J.; Wen, X.; Tang, Q.; Liu, D.; Chen, S. An Innovative Waterwheel-Rotating Biological Contactor (WRBC) System for Rural Sewage Treatment. *Water* **2023**, *15*, 1323. [CrossRef]
2. Mahmood, Q.; Zheng, P.; Cai, J.; Wu, D.; Hayat, Y.; Hassan, M.J. Anoxic sulfide biooxidation using nitrite as an electron acceptor. *J. Hazard. Mater.* **2007**, *147*, 249–256. [CrossRef] [PubMed]
3. Mahmood, Q.; Zheng, P.; Cai, J.; Wu, D. Sulfide removal through simultaneous nitrogen and sulfur cycles in an anoxic bioreactor. *Bioresour. Technol.* **2007**, *98*, 2550–2557. [CrossRef]
4. Mahmood, Q.; Zheng, P.; Cai, J.; Wu, D. Simultaneous removal of sulfide and nitrate in anaerobic baffled reactor. *J. Hazard. Mater.* **2008**, *150*, 835–841. [CrossRef]
5. Mahmood, Q.; Zheng, P.; Cai, J.; Wu, D.; Hayat, Y.; Hassan, M.J.; Azim, M.R. Prediction of simultaneous sulfide and nitrate removal from wastewater using an artificial neural network (ANN) model. *J. Hazard. Mater.* **2009**, *164*, 1023–1030. [CrossRef]
6. Zhang, Y.; Wu, P.; Zhao, X.; Jin, Y. Advanced insights into integrated nitrogen and sulfur removal processes: New findings and engineering applications. *Water* **2025**, *17*, 411.
7. Wang, Z.B.; Zhang, J.; Miao, Q.; Cao, H.Y.; Xiong, F.; Lee, T.; El-Baz, A.; Xie, L.; Ni, S.Q. Achieving Stable Partial Denitrification by Selective Inhibition of Nitrite Reductase with the Biosafe Aprotic Solvent DMSO. *Environ. Sci. Technol.* **2024**, *58*, 21242–21250. [CrossRef]
8. Jing, H.; Tan, J.; Zhao, J.; Zhou, L. Sulfide removal from wastewater: A review focusing on technologies and operational strategies. *Bioresour. Technol.* **2007**, *98*, 1067–1073. [CrossRef]

9. Jing, H.; Tan, J.; Zhao, J.; Zhou, L. Nitrite-driven sulfide oxidation processes: From fundamentals to applications. *Water Res.* **2008**, *42*, 3303–3312. [CrossRef]
10. Cai, J.; Sun, Y.; Qaisar, M.; Wang, K.; Chen, B. Revealing the Effect of Multiple Nitrogen Sources on Sulfide Oxidation by Progressively Changing Nitrate to Nitrite. *Sep. Purif. Technol.* **2022**, *283*, 120226. [CrossRef]
11. Jing, H.; Tan, J.; Zhao, J.; Zhou, L. Microbial communities involved in sulfide oxidation coupled with nitrogen removal processes: Current knowledge and future perspectives. *Water Res.* **2015**, *68*, 595–607. [CrossRef]
12. Wang, J.; Zhang, Y.; Liu, Y. Sulfide oxidation coupled to nitrate and nitrite reduction: Mechanisms and microbial communities. *Water Res.* **2022**, *217*, 118404. [CrossRef]
13. Wang, J.; Zhang, Y.; Liu, Y. Advances in sulfide removal biotechnologies: New perspectives for high-salinity wastewater treatment. *Water* **2022**, *14*, 3407. [CrossRef]
14. Gupta, P.; Raza, M.Q. Recent advances in neural network modeling for water and wastewater treatment processes. *Water* **2019**, *11*, 2051. [CrossRef]
15. Zou, H.; Hastie, T. Regularization and variable selection via the elastic net. *J. R. Stat. Soc. Ser. B* **2005**, *67*, 301–320. [CrossRef]
16. Almeida, P.E.M. Neural networks in chemical engineering. *Chem. Eng. Technol.* **2002**, *25*, 615–621.
17. Huang, G.-B. Learning capability and storage capacity of two-hidden-layer feedforward networks. *IEEE Trans. Neural Netw.* **2003**, *14*, 274–281. [CrossRef]
18. Rogers, S.K.; Dowla, F.U. *Neural Network Methods for Solving Partial Differential Equations*; MIT Press: Cambridge, MA, USA, 1994.
19. Jing, H.; Tan, J.; Zhao, J.; Zhou, L. Feature learning for prediction tasks in wastewater treatment processes. *Bioresour. Technol.* **2017**, *243*, 1081–1089. [CrossRef]
20. Nassif, A.B.; Shahin, I.; Attili, I.; Azzeh, M.; Shaalan, K. Speech recognition using deep neural networks: A systematic review. *IEEE Access* **2019**, *7*, 19143–19165. [CrossRef]
21. Goldberg, Y. A primer on neural network models for natural language processing. *J. Artif. Intell. Res.* **2016**, *57*, 345–420. [CrossRef]
22. Kebria, D.Y.; Bakhshipour, A.; Mohammadi, A. A review of deep learning approaches for autonomous driving. *J. Adv. Transp.* **2019**, *2019*, 9324092.
23. Papik, K.; Molnár, B.; Schaefer, E.; Dombovári, Z.; Tulassay, Z.; Fehér, J. Application of neural networks in medicine—A review. *Med. Sci. Monit.* **1998**, *4*, 538–546.
24. Ge, Z.; Song, Z.; Ding, S.X.; Huang, B. Data mining and analytics in the process industry: The role of machine learning. *IEEE Access* **2017**, *5*, 20590–20616. [CrossRef]
25. Uzair, M.; Jamil, A. Understanding Artificial Neural Networks for Environmental Predictions. *Water* **2020**, *12*, 1478. [CrossRef]
26. Ryo, M.; Angelov, B.; Mammola, S.; Kass, J.M.; Benito, B.M.; Hartig, F. Explainable artificial intelligence enhances the ecological interpretability of black-box species distribution models. *Ecography* **2021**, *44*, 199–205. [CrossRef]
27. Arashpour, M. AI explainability framework for environmental management research. *J. Environ. Manag.* **2023**, *342*, 118149. [CrossRef]
28. Park, J.; Lee, W.H.; Kim, K.T.; Park, C.Y.; Lee, S.; Heo, T.Y. Interpretation of ensemble learning to predict water quality using explainable artificial intelligence. *Sci. Total Environ.* **2022**, *832*, 155070. [CrossRef]
29. Alshehri, F.; Rahman, A. Coupling machine and deep learning with explainable artificial intelligence for improving prediction of groundwater quality and decision-making in Arid Region, Saudi Arabia. *Water* **2023**, *15*, 2298. [CrossRef]
30. Mallick, J.; Alqadhi, S.; Hang, H.T.; Alsubih, M. Interpreting optimised data-driven solution with explainable artificial intelligence (XAI) for water quality assessment for better decision-making in pollution management. *Environ. Sci. Pollut. Res.* **2024**, *31*, 42948–42969. [CrossRef] [PubMed]
31. Infant, S.S.; Vickram, A.S.; Saravanan, A.; Muthu, C.M.; Yuarajan, D. Explainable Artificial Intelligence for Sustainable Urban Water Systems Engineering. *Results Eng.* **2025**, *25*, 104349. [CrossRef]
32. Nasir, F.B.; Li, J. Understanding machine learning predictions of wastewater treatment plant sludge with explainable artificial intelligence. *Water Environ. Res.* **2024**, *96*, e11136. [CrossRef] [PubMed]
33. Al Saleem, M.; Harrou, F.; Sun, Y. Explainable machine learning methods for predicting water treatment plant features under varying weather conditions. *Results Eng.* **2024**, *21*, 101930. [CrossRef]
34. Park, J.; Ahn, J.; Kim, J.; Yoon, Y.; Park, J. Prediction and interpretation of water quality recovery after a disturbance in a water treatment system using artificial intelligence. *Water* **2022**, *14*, 2423. [CrossRef]
35. Martini, A.; Karmonik, C.; Narayana, P.A. Application of SHAP (Shapley Additive Explanations) values for model interpretability in healthcare. *Healthcare* **2021**, *9*, 1324. [CrossRef]
36. Jia, X.; Yang, Y.; Guo, S.; Yang, F.; Zeng, H. Shapley value methods for explaining feature importance in machine learning models. *Knowl.-Based Syst.* **2019**, *195*, 105746. [CrossRef]
37. Ghalebikesabi, S.A.; Grolinger, K.; Capretz, M.A.M. Explainable machine learning for smart manufacturing: A SHAP approach. *Sensors* **2021**, *21*, 6325. [CrossRef]

38. Bartsch, T.; Soave, N. Multiple normalized solutions for a competing system of Schrödinger equations. *Calc. Var. Partial Differ. Equ.* **2019**, *58*, 22. [CrossRef]
39. Janssen, A.J.H.; Ma, S.C.; Lens, P.; Lettinga, G. Performance of a sulfide oxidizing expanded bed reactor supplied with dissolved oxygen. *Biotechnol. Bioeng.* **1997**, *53*, 32–40. [CrossRef]
40. Zhang, L.; Mu, Y.; Chen, Y.; Lu, X.; Song, R. Study on Synergistic Desulfurization and Chlorine Resistance of Alkaline Metal Oxides@ ZrO2/γ-Al2O3-Loaded Catalysts. *Adv. Eng. Mater.* **2025**, *27*, 2500654. [CrossRef]
41. McNeice, J.A. Biogenic Thiosulfate Production for Gold Leaching. Ph.D. Thesis, Queen's University, Kingston, ON, Canada, 2023.
42. Sun, Y.; Qaisar, M.; Wang, K.; Chen, B.; Cai, J. Validation of Effective Role of Substrate Concentrations on Elemental Sulfur Generation in Simultaneous Sulfide and Nitrate Removal Process. *Sep. Purif. Technol.* **2021**, *268*, 118698. [CrossRef]
43. Yuan, Y.; Huang, Y.; Li, X.; Wang, L. Operation factors of autotrophic denitrification with elemental sulfur as terminal product. *Appl. Mech. Mater.* **2013**, *295–298*, 1110–1114. [CrossRef]
44. Chu, Y.; Zhang, X.; Tang, X.; Jiang, L.; He, R. Uncovering anaerobic oxidation of methane and active microorganisms in landfills by using stable isotope probing. *Environ. Res.* **2025**, *271*, 121139. [CrossRef] [PubMed]
45. Sublette, K.L.; Kolhatkar, R.; Raterman, K. Technological aspects of the microbial treatment of sulfide-rich wastewaters: A case study. *Biodegradation* **1998**, *9*, 259–271. [CrossRef] [PubMed]
46. Coha, M.; Farinelli, G.; Tiraferri, A.; Minella, M.; Vione, D. Advanced oxidation processes in the removal of organic substances from produced water: Potential, configurations, and research needs. *Chem. Eng. J.* **2021**, *414*, 128668. [CrossRef]
47. Tao, L.; Wu, H.; Wang, J.; Li, B.; Wang, X.Q.; Ning, P. Removal of SO_2 from flue gas using Bayer red mud: Influence factors and mechanism. *J. Cent. South Univ.* **2019**, *26*, 467–478. [CrossRef]
48. Sublette, K.L. Microbial treatment of sour gases for the removal and oxidation of hydrogen sulfide. *Gas Sep. Purif.* **1990**, *4*, 91–96. [CrossRef]
49. Li, H.; Tao, Y.; Xu, T.; Wang, H.; Yang, M.; Chen, Y.; Wang, A. Real-time quantification of activated sludge concentration and viscosity through deep learning of microscopic images. *Environ. Sci. Ecotechnol.* **2025**, *24*, 100527. [CrossRef]

Disclaimer/Publisher's Note: The statements, opinions and data contained in all publications are solely those of the individual author(s) and contributor(s) and not of MDPI and/or the editor(s). MDPI and/or the editor(s) disclaim responsibility for any injury to people or property resulting from any ideas, methods, instructions or products referred to in the content.